Universidade de Lisboa
Faculdade de Farmácia

Functional analysis of signaling pathways activated by Toll-like receptor 2 heterodimers

Mariana da Fonseca Ramos Lisboa

Trabalho de Campo orientado pelo Professor Doutor Günther Weindl, Professor Associado, da Universidade de Bona e coorientado pela Professora Doutora Elsa Margarida Teixeira Rodrigues, Professora Associada, da Faculdade de Farmácia da Universidade de Lisboa

Mestrado Integrado em Ciências Farmacêuticas

2024

Universidade de Lisboa

Faculdade de Farmácia

Functional analysis of signaling pathways activated by Toll-like receptor 2 heterodimers

Mariana da Fonseca Ramos Lisboa

Trabalho Final de Mestrado Integrado em Ciências Farmacêuticas apresentado à Universidade de Lisboa através da Faculdade de Farmácia

Trabalho de Campo orientado pelo Professor Doutor Günther Weindl, Professor Associado, da Universidade de Bona e coorientado pela Professora Doutora Elsa Margarida Teixeira Rodrigues, Professora Associada, da Faculdade de Farmácia da Universidade de Lisboa

2024

Acknowledgments

I want to express my gratitude for Professor Doctor Gunther Weindl for welcoming me into his research group and enabling me to take my first steps in my research career. It was three months filled with challenges and learning experiences that have contributed to my personal and professional growth, and I am very thankful for the opportunity. I would also like to express my gratitude to Professor Doctor Elsa Rodrigues for her support throughout my research. Her insightful discussions, guidance, and the transparent way she co-supervised my thesis have profoundly impacted my work.

A special thanks goes to Felicitas Lauber for her warm reception and for seamlessly integrating me into her research work. I really appreciate the knowledge she shared, which was essential in the completion of this project. Her patience in addressing my questions and her willingness to assist me whenever I needed help made a significant difference in my experience. I would also like to extend my gratitude to the entire Bonn lab team for their warm welcome and support.

Finally, I cannot forget to thank my parents, sister, and brother, who are the most important people in my life. Thank you for being my pillars of support, for listening to my frustrations, and for standing by me when I needed it most.

Declaro ter desenvolvido e elaborado o presente trabalho em consonância com o Código de Conduta e de Boas Práticas da Universidade de Lisboa. Mais concretamente, afirmo não ter incorrido em qualquer das variedades de fraude académica, que aqui declaro conhecer, e que atendi à exigida referenciação de frases, extratos, imagens e outras formas de trabalho intelectual, assumindo na íntegra as responsabilidades da autoria.

Resumo

Os recetores do tipo Toll (TLR) são componentes do sistema imunitário inato, responsáveis pelo reconhecimento de padrões moleculares associados a agentes patogénicos (PAMPs) e pelo início de respostas imunitárias. Este estudo tem como objetivo estudar a ativação diferencial dos heterodímeros TLR2 por ligandos específicos e a ativação de vias de sinalização a jusante em diferentes linhas celulares.

Utilizámos células repórter HEK-Blue concebidas para expressar especificamente TLR2/1, TLR2/6 ou TLR4, de modo a avaliar as suas respostas funcionais a extratos de *Escherichia coli* (HKEB), e de *Staphylococcus aureus* (HKSA) preparados a partir de bactérias mortas pelo calor. A análise de Western blot demonstrou padrões de expressão distintos das proteínas adaptadoras TRIF e My-D88, o que mostra a adequada utilização das linhas celulares selecionadas para estudar a sinalização dos recetores do tipo Toll. Posteriormente, os nossos resultados indicaram que os heterodímeros TLR2/1 apresentaram maior atividade em resposta a HKEB, enquanto os heterodimeros TLR2/6 foram preferencialmente ativados por HKSA. Adicionalmente, o TLR4 foi exclusivamente responsivo à HKEB, confirmando o seu papel como recetor primário a componentes bacterianos Gram-negativos. Nos queratinócitos HaCaT, observámos um aumento significativo na secreção de IL-8 após estimulação com HKSA, particularmente em concentrações mais elevadas, sugerindo que estas células são mais sensíveis a componentes bacterianos Gram-positivos.

Os nossos resultados mostram que os modelos *in vitro* escolhidos podem ser utilizados para o rastreio de ligandos específicos para os diferentes TLR com o objetivo de ajudar a melhorar a nossa compreensão acerca da especificidade da sinalização TLR e das funções únicas de TRIF e MYD88 em diferentes contextos celulares. Estes resultados têm implicações significativas para o desenvolvimento de imunoterapias e vacinas direcionadas para agentes patogénicos específicos. Embora o nosso estudo ofereça um contributo para este domínio, são essenciais estudos *in vivo* para validar estes mecanismos.

Em resumo, esta investigação elucida a complexa interação entre os TLR e as suas proteínas adaptadoras na formação de respostas imunitárias a agentes patogénicos bacterianos, lançando as bases para futuros estudos destinados a melhorar as estratégias terapêuticas em doenças infeciosas.

Palavras-chave: Imunidade inata, Recetores do tipo Toll, Vias de sinalização imunitária, Células repórter HEK-Blue.

Abstract

Toll-like receptors are integral components of the innate immune system, responsible for recognizing pathogen-associated molecular patterns (PAMPs) and initiating immune responses. This study aims to investigate the differential activation of TLR2 heterodimers by specific ligands, and the activation of downstream signaling pathways across various cell types.

We utilized HEK-Blue reporter cells engineered to specifically express TLR2/1, TLR2/6 or TLR4, to assess their functional responses to heat-killed *Escherichia coli* (HKEB) and *Staphylococcus aureus* (HKSA). Western blot analysis demonstrated distinct expression patterns of TRIF and My-D88 adaptor proteins, which show the adequacy of the chosen cell lines, to study TLR signaling. Afterwards, our results indicated that TLR2/1 heterodimers showed higher activity in response to HKEB, while TLR2/6 receptors were preferentially activated by HKSA. Notably, TLR4 was exclusively responsive to HKEB, confirming its role as a primary receptor for Gram-negative bacterial components. In HaCaT keratinocytes, we observed a significant increase in IL-8 secretion upon stimulation with HKSA, particularly at higher concentrations, suggesting that these cells are more responsive to Gram-positive bacterial components. This IL-8 response is indicative of TLR2-mediated signaling, emphasizing the skin's innate immune capacity to respond to pathogens commonly associated with skin infections.

Our results show that the *in vitro* models chosen, can be used for high-throughput screening of specific TLR ligands, and will help to enhance our understanding of TLR signaling specificity and the unique functions of TRIF and MYD88 in different cellular contexts. Moreover, these findings have significant implications for the development of targeted immunotherapies and vaccines to specific pathogens. While the study offers valuable contributions to the field, further *in vivo* investigations are essential to validate these mechanisms and refine our understanding of TLR signaling dynamics across diverse tissue types and environments.

In summary, this research elucidates the complex interplay between TLRs and their adaptor proteins in shaping immune responses to bacterial pathogens, laying the groundwork for future studies aimed at improving therapeutic strategies in infectious diseases.

Keywords: Innate immunity, Toll-like receptors, Immune signaling pathways, HEK-Blue reporter cells

Abbreviations

DAMP - Damaged associated molecules pattern

DCs - Dendritic cells

HKEB - Heat Killed Escherichia coli

HKSA - Heat Killed Staphylococcus aureus

IFN - Interferon

IL - Interleukin

IRF - Interferon regulatory factor

LPS - bacterial lipopolysaccharide

LRR - Leucine-rich repeats

LTA - Lipoteichoic acid

MAPK - Mitogen-activated protein kinases

MyD88 - Myeloid differentiation primary-response protein 88

NK - Natural Killer

NF-κB - Nuclear factor-kappa B

NLR - Nod-like receptor

PAMP - Pathogen-associated molecular pattern

PRR - Pattern recognition receptor

TIRAP - Toll-interleukin 1 receptor (TIR) domain-containing adaptor protein

TLR - Toll-like receptor

TRAF - Tumor necrosis factor receptor-associated factor

TRAM - TRIF-related adaptor molecule

TIR - Toll/IL-1 receptor

TRIF - TIR-domain-containing adaptor inducing interferon-β

Table of Contents

List of Figures

List of Tables

1. Introduction

1.1 The Immune System

Humans and other mammals host a diverse array of microbes. The microbial community includes obligate pathogens that must be controlled to prevent disease, along with commensal and mutualistic organisms that play a crucial role in maintaining healthy tissues and organ function. Pathogenic microbes employ various strategies to replicate, spread, and disrupt normal host functions. While the immune system uses powerful effector mechanisms to eliminate these harmful microbes and neutralize toxic or allergenic substances, it must also avoid causing excessive damage to the host's own tissues or inadvertently destroying beneficial commensal microbes. The ability of the immune system to avoid attacking self-tissues is known as self-tolerance. It is now well-established that both the innate and adaptive immune responses possess mechanisms to prevent immune reactions against self-antigens (1).

Traditionally, host immunity is categorized into innate and adaptive responses. Innate immunity acts quickly and non-specifically against pathogens, providing an immediate defence. In contrast, adaptive immunity responds more slowly but with high specificity, creating long-lasting immunological memory (2). During an infection, the innate immunity is the first to be triggered, taking no longer than minutes to hours to be fully activated (3). This is crucial for the host defence in the first phase of a new infection. While innate immunity is generally able to eliminate the pathogens efficiently, initial clearance of infection can fail due to the high number or virulence of invading pathogens. In these situations, lymphocytes and adaptive immune mechanisms are activated, which allows specific recognition and elimination of the pathogen. The development of adaptive immunity takes 1–2 weeks and plays a critical role in host defence during the later stages of an infection, as well as in secondary infections. Its ability to "remember" pathogens enables a faster and more effective response upon re-exposure (2).

1.2 Innate immunity response

The innate immune response serves as the body's first line of defence against invading pathogens. It includes several physical barriers, such as epithelial cell layers with tightly connected cells that prevent pathogen entry, along with proteins and bioactive molecules present in biological fluids like mucus and saliva. If a pathogen breaches these barriers, both hematopoietic (blood-derived) and non-hematopoietic cells are activated in response to the damage or infection (1). Most cells involved in the innate immune response are of hematopoietic origin, including macrophages, dendritic cells, neutrophils, and natural killer (NK) cells. However, epithelial and parenchymal cells also play a crucial role by producing

enzymes and antimicrobial peptides that help neutralize pathogens. Additionally, these cells secrete chemokines to attract granulocytes (such as neutrophils) and T cells to the site of infection (1). One of the key components of this early response is the recruitment of neutrophils from the bloodstream. In response to inflammatory signals, such as chemotactic factors and cytokines, neutrophils quickly move to the infection site. They then recognize and ingest (phagocytose) pathogens that have been opsonized, or marked for destruction, by antibodies or components of the complement system. Once inside the neutrophil, pathogens are destroyed through a variety of cytotoxic mechanisms, which include the release of enzymes, reactive oxygen species, and other antimicrobial agents (1).

The innate immune system employs germline-encoded pattern recognition receptors (PRRs) for the initial detection of microbes. PRRs recognize microbe-specific molecular signatures known as pathogen-associated molecular patterns (PAMPs) and self-derived molecules derived from damaged cells, referred to as damage associated molecular patterns (DAMPs). Upon the recognition of their specific ligands from the invasive pathogens or damaged cells, PRRs initiate a variety of downstream signaling cascades, including nuclear factor kappa B (NF-κB), type I interferon (IFN) and inflammasome signaling pathways, leading to the production of corresponding proinflammatory or antiviral cytokines and chemokines (4,5). Therefore, PRRs are a key element of the immune system and include the Toll-like receptors (TLRs), RIG-I-like receptors, Nod-like receptors (NLRs), AIM2-like receptors, C-type lectin receptors, and intracellular DNA and RNA sensors (4–7). The activation of TLR signaling is also crucial to the induction of antigen-specific adaptive immune responses by promoting the maturation of dendritic cells (DCs) and activating the adaptive immune cells for the clearance of invading pathogens (4,8,9). These responses are essential for the clearance of infecting microbes as well as crucial for the consequent instruction of antigen-specific adaptive immune responses (9).

1.3 Toll like receptors

As mentioned before, mammals have several distinct classes of PRRs. Among these, TLRs were the first to be identified, and are the best characterized. The TLR family comprises 10 members (TLR1–TLR10) in humans and 12 (TLR1–TLR9, TLR11–TLR13) in mice. Each TLR is composed of an ectodomain with leucine-rich repeats (LRRs) that mediate PAMPs recognition, a transmembrane domain, and a cytoplasmic Toll/IL-1 receptor (TIR) domain that initiates downstream signaling. The ectodomain displays a horseshoe-like structure, and TLRs interact with their respective PAMPs or DAMPs as a homo- or heterodimer along with a co-receptor or accessory molecule (9,10).

TLRs are expressed in innate immune cells such as dendritic cells and macrophages as well as non-immune cells such as fibroblast cells and epithelial cells. TLRs are largely classified into two subfamilies based on their localization: cell surface TLRs and intracellular TLRs. Cell surface TLRs include TLR1, TLR2, TLR4, TLR5, TLR6, and TLR10, whereas intracellular TLRs, localized in the endosome include TLR3, TLR7, TLR8, TLR9, TLR11, TLR12 and TLR13 (9,11). Cell surface TLRs mainly recognize microbial membrane components such as lipids, lipoproteins and proteins while intracellular TLRs mainly recognize microbial nucleic acids derived from bacteria and viruses and recognize self-nucleic acids in disease conditions such as autoimmunity (12). Specifically, TLR4 recognizes bacterial lipopolysaccharide (LPS), TLR2 along with TLR1 or TLR6 recognizes a wide variety of PAMPs including lipoproteins, peptidoglycans, lipotechoic acids or tGPI-mucin and TLR5 recognizes bacterial flagellin. Conversely, TLR3 recognizes viral double-stranded RNA (dsRNA), small interfering RNAs, and self-RNAs derived from damaged cells, while TLR7 is predominantly expressed in plasmacytoid DCs (pDCs) and recognizes single stranded RNA (ssRNA) from viruses. Human TLR8 responds to viral and bacterial RNA (**Figure 1**) (9,11,13,14).

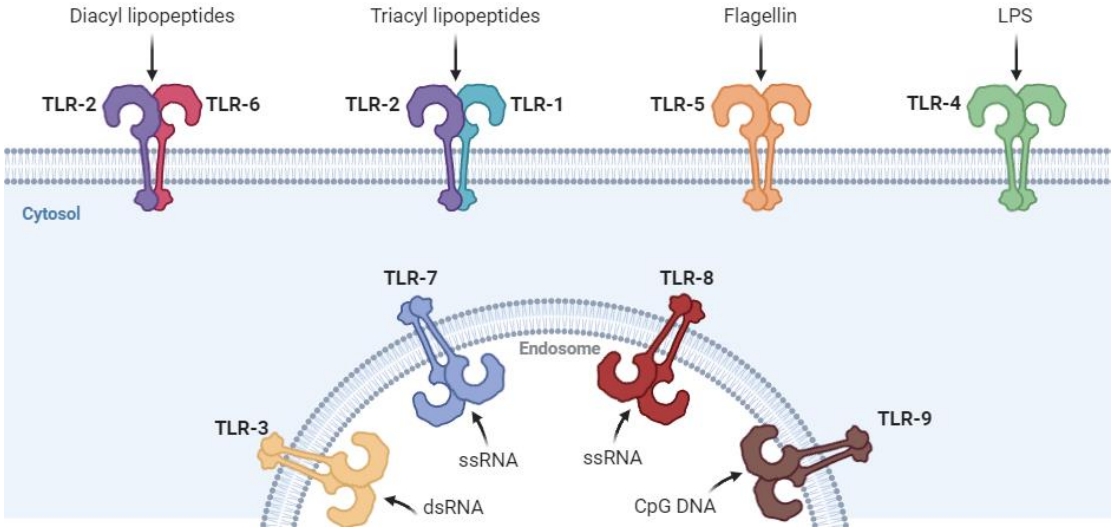

Figure 1. Location and ligand specificity of Toll-like receptors involved in immune response.

Cell surface TLRs, including TLR2/6, TLR2/1, TLR5, and TLR4, detect microbial components such as diacylated lipopeptides, triacylated lipopeptides, flagellin, and LPS, respectively. In endosomes, TLR3 recognizes double-stranded RNA, TLR7 and TLR8 bind single-stranded RNA, and TLR9 detects unmethylated CpG DNA. These receptors enable the immune system to identify diverse pathogens and initiate immune responses. Image produced by BioRender.

As transmembrane proteins, all TLRs are synthesized in the endoplasmic reticulum, transported to the Golgi, and are recruited to the cell surface or to intracellular compartments. Intracellular localization of TLRs is thought to be critical for ligand recognition as well as for

preventing TLRs from encountering self-nucleic acids, which could cause autoimmunity (9,15,16).

1.4 Toll like receptors signaling pathways

Upon PAMPs and DAMPs recognition, TLRs recruit Toll/interleukin-1 receptor/resistance protein (TIR) domain-containing adaptor proteins such as Myeloid Differentiation Primary Response 88 (MyD88) and TIR domain-containing adaptor protein inducing interferon beta (TRIF), which initiate signal transduction pathways that culminate in the activation of NF-κB, Interferon regulatory factors (IRF), or Mitogen-activated protein kinases (MAPK) to regulate the expression of cytokines, chemokines, and type I IFNs that ultimately protect the host from microbial infection (9). MyD88 activates NF-κB and MAPKs for the induction of inflammatory cytokine genes. TRIF is recruited to TLR3 and TLR4 and promotes an alternative pathway that leads to the activation of IRF3, NF-κB, and MAPKs for induction of type I IFN and inflammatory cytokine genes. TRAM (TRIF-related adaptor molecule) is selectively recruited to TLR4 but not TLR3 to link between TRIF and TLR4 (9,17,18). Collectively, depending on the adaptor usage, TLR signaling is largely divided into two pathways: the MyD88-dependent and TRIF-dependent pathways (9).

1.4.1 The MyD88-dependent pathway

The MYD88- dependent pathway is utilized by all TLRs (except TLR3) which eventually lead to the enhanced expression of proinflammatory cytokine genes. MyD88 recruitment to the activated C-terminal domain of the TLRs is facilitated by two important adaptor molecules - Myelin and lymphocyte protein (MAL) and TIR domain containing adaptor protein (TIRAP). Mal adaptor protein is utilized by all kinds of TLR receptors to recruit MyD88, while TLR1, 2, 4, and 6 require additional association with TIRAP to facilitate the contact with MyD88 (19).

Upon TLR activation, MyD88 uses its death domain to interact with the death domains of IRAK (IL-1 receptor-associated kinase) family members, including IRAK1, IRAK2, IRAK4, and IRAK-M (20). Initially, IRAK4 is activated and has an essential role in the activation of NF-κB and MAPK downstream of MyD88. Afterwards, IRAK4 activates IRAK1, which is then autophosphorylated at several sites and released from MyD88 (21). Once IRAK4 and IRAK1 have been sequentially phosphorylated, they detach from MyD88 and bind to TRAF6. TRAF6, in cooperation with E2 enzymes (Ubc13 and Uev1A), promotes Lysine 63-linked polyubiquitination of target proteins, including itself and NEMO (NF-κB essential modifier, also known as IKKγ) (20,22). This type of ubiquitination facilitates protein-protein interactions and is crucial for activating downstream signaling pathways and regulating subcellular localization. Ubiquitinated NEMO and TRAF6 then recruit a protein kinase complex composed of TAK1

(transforming growth factor-beta-activated kinase-1) and TAK1-binding proteins (TAB1, TAB2, and TAB3), which initiates two main signaling branches: the IKK complex-NF-κB pathway and the mitogen-activated protein kinase (MAPK) pathway (involving ERK, JNK, and p38) (20,23,24). The activation of the MyD88-dependent pathway results in the induction of many genes, and some of these have critical roles in modulating NF-κB-dependent transcription (11).

In TLR signaling, the most activated NF-κB complex is a heterodimer of RelA and p50, which remains in the cytoplasm as an inactive form bound to IκB proteins in unstimulated cells (20). TLR ligand stimulation rapidly triggers phosphorylation of specific serine residues in IκB by the IKK complex—a multiprotein complex comprising two catalytic components (IKKα and IKKβ) and a regulatory component, NEMO. Both IKKα and IKKβ contain a kinase domain, a leucine zipper domain, helix-loop-helix structures, and a NEMO-binding domain (NBD) (20). Phosphorylated IκB is then polyubiquitinated and degraded by the 26S proteasome, freeing NF-κB to translocate into the nucleus. This cascade, known as the "canonical pathway," is responsible for the TLR-induced production of inflammatory cytokines, such as tumor necrosis factor-alpha (TNF-α) and interleukin-6 (IL-6) (20). Genetic studies have demonstrated that IKKβ, rather than IKKα, is crucial for NF-κB activation in TLR signaling. Conversely, IKKα's kinase activity appears to play a role in terminating NF-κB activation, helping regulate the duration of the immune response (25) **(Figure 2)**.

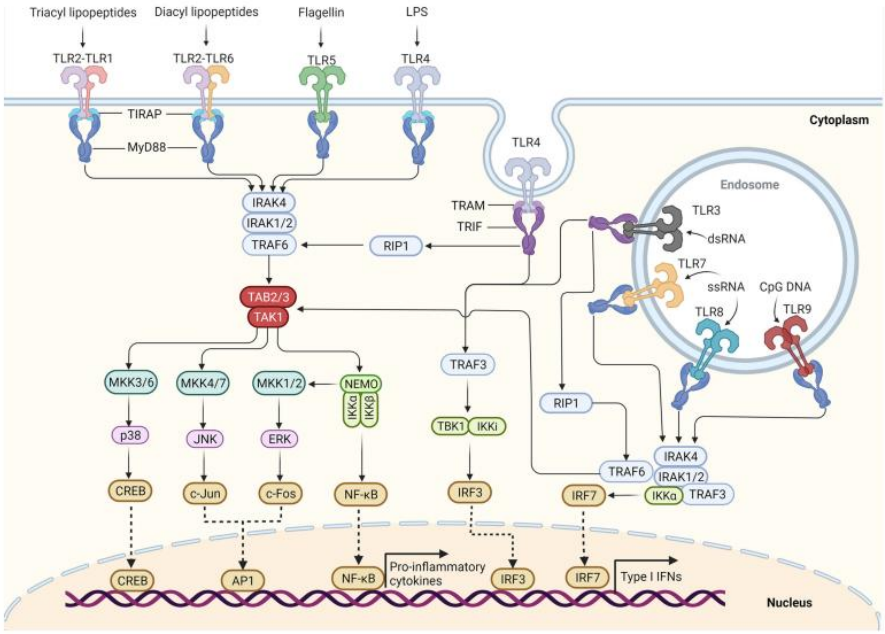

Figure 2. Toll-Like Receptor Signaling Pathways and Their Role in Inflammatory Responses.

TLRs recognize specific pathogen-associated molecular patterns (PAMPs). Signal transduction involves adaptor proteins (e.g. MyD88, TRIF) and downstream kinases (e.g. IRAKs, TAK1), leading to activation of transcription factors (e.g. NF-κB, AP-1, IRFs). This results in the production of pro-inflammatory cytokines and type I interferons, contributing to the immune response (4).

1.4.2 The TRIF-dependent pathway

The TRIF-dependent pathway is utilized by TLR3 and TLR4 to trigger the enhanced expression of interferon type-1 genes. TLR3 utilizes it in response to the binding of viral dsRNA by recruiting TRIF directly, while TLR4 requires another adaptor protein, TRAM, for the activation of TRIF (6,19). TRIF interacts with TRAF6 and TRAF3 and TRAF6 recruits the kinase RIP-1, which in turn interacts with and activates the TAK1 complex, leading to activation of NF-κB and MAPKs and induction of inflammatory cytokines. In contrast, TRAF3 recruits the IKK-related kinases TBK1 and IKKi along with NEMO for IRF3 phosphorylation. Subsequently, IRF3 forms a dimer and translocates into the nucleus from the cytoplasm, where it induces the expression of type I IFN genes (5,11). The Pellino family E3 ubiquitin ligases are implicated in TLR signaling (26). Pellino-1-deficient mice display impaired TRIF-dependent NF-κB activation and cytokine production (27). Pellino-1 is phosphorylated by TBK1/IKKi and thereby facilitates ubiquitination of RIP-1, suggesting that Pellino-1 mediates TRIF-dependent NF-κB activation by recruiting RIP-1. Furthermore, Pellino-1 regulates IRF3 activation by binding to DEAF-1, a transcription factor that facilitates binding of IRF3 to the IFNβ promoter (26) **(Figure 2)**.

Therefore, TLR4 activates both the MyD88-dependent and TRIF-dependent signaling pathways. In contrast, TLR2 heterodimers predominantly initiate MyD88-dependent signaling pathways, with limited evidence supporting their role in TRIF-dependent signaling (9,28,29).

1.5 TLR2 Heterodimers and Ligands

TLR2, along with TLR4, is one of the most studied pattern recognition receptors, and unlike certain other receptors in this family, TLR2 is known to form various heterodimers with TLR1, TLR4, TLR6, and TLR10 (30–32). In recent years, a growing number of studies have shown that TLR2 may be the most versatile TLR, as this receptor recognizes a broad repertoire of ligands from a variety of pathogen sources and interacts with many other receptors (29,30,33). This ability of TLR2 to dimerize, greatly expands the spectrum of detectable pathogens. Structural studies of the heterodimers have supported the importance of ligand binding to stabilize TLR2/1 and TLR2/6 dimerization for downstream signaling (30,34,35).

TLR2/1 heterodimers can sense triacylated lipopeptides (LPs) from Gram-negative bacteria or mycoplasma, whereas TLR2/6 heterodimers recognize diacylated LPs, including lipoteichoic acid (LTA) from Gram-positive bacteria and mycoplasma. (29,30,36,37). Additional co-receptors, such as clusters of differentiation 14 (CD14), have been described to bring TLR2 and TLR1 into physical proximity by binding LPs to induce signaling (30,38). Besides heterodimerization, some evidence also points to the existence of TLR2 homodimerization, but this is still controversially discussed (29,30,39). Commonly used TLR2 ligands for *in vitro* and *in vivo* studies are synthetic di- and triacylated LPs such as Pam2CSK4, Pam3CSK4, isolated

from *Escherichia coli*, and FSL-1, which represents a PAMP of the LP isolated from *Mycoplasma fermentans* or *Mycoplasma salivarium* (29,30,40,41). Moreover, endogenous ligands, danger signals for TLR2, have been identified, including heat shock proteins, human β-defensin-3, high mobility group box 1 protein (HMGB1), and hyaluronan fragments (30,42–44). Therefore, in addition to PAMPs, endogenous TLR2 activation by host-derived danger signals is a viable factor in the pathogenesis of inflammation and related diseases.

The major TLR2 ligands characterized thus far are lipoproteins, ubiquitous to all bacteria and highly expressed in the outer membrane of Gram-positive bacteria. They present a unique NH3-terminal lipo-amino acid, N-acyl-S-diacylglycerol cysteine and usually three lipid chains (triacyl), except for those found in mycobacteria that can have two lipid chains (diacyl). No matter which of the two dimers is activated, the classical signaling cascade triggered was found to be the same. TLR2 primarily relies on the MyD88 and TIRAP adaptors for signaling (30,45,46).

2. Aim

The primary aim of this study is to investigate the mechanisms by which TLR protein agonists modulate innate immune signaling pathways. Understanding these mechanisms is essential, as TLRs play a crucial role in initiating immune responses and defending against pathogens. This research specifically focuses on the following objectives:

a) Determine the Expression levels of Key Proteins in TLR Signaling: Protein lysates from HEK Blue hTLR4, HEK Blue hTLR2/1, HEK Blue hTLR2/6, HaCaT keratinocytes, THP-1 monocytes, and HEK293 cells were prepared, and analysed by Western blot analysis, to determine the expression of MyD88 and TRIF, which are essential adaptor proteins involved in TLR signaling. By comparing expression patterns across cell types, we will elucidate the differential roles of MyD88- and TRIF-mediated pathways in immune and non-immune cells, providing insight into cell-specific signaling responses.

b) Characterize Dose-Response Profiles of TLR2/1, TLR2/6 and TLR4 Agonists: To define specific activation profiles, the response to increasing concentrations of TLR agonists, namely heat-killed *Staphylococcus aureus* (HKSA) and heat-killed *Escherichia coli* (HKEB) were analysed in HEK-blue reporter cells expressing human TLR4 (hTLR4), human TLR2/1, and human TLR2/6. This allows to assess receptor-specific cellular responses to different ligands.

c) Examine Cytokine Production in Keratinocytes Exposed to Gram-Positive and Gram-Negative Bacterial Components: HaCaT cells were stimulated with various doses of TLR ligands, specifically HKSA and HKEB, to measure IL-8 secretion and assess differential cytokine responses.

Together, these objectives aim to deepen our understanding of TLR2-mediated immune responses and clarify the roles of the MYD88 and TRIF pathways, potentially informing therapeutic strategies for immune-related diseases.

3. Materials and Methods

3.1 Materials

In this section a comprehensive list of laboratory equipment (Table I), consumables (Table II), chemicals and reagents (Table III), cell culture medium and supplements (Table IV), antibodies (Table V) and software (Table VI) used is presented.

3.1.1 Laboratory Equipment

Table I. List of laboratory equipment

Equipment	Model	Manufacturer
Cell counter	Luna II automated cell counter	BioCat GmbH, Germany
Centrifuge	Allegra™ 25R	Beckman Coulter GmbH, Germany
Centrifuge	5417R	Eppendorf, Germany
Freezer -80 °C	CryoCube F101h	Eppendorf, Germany
Incubator	Binder Cell Incubator CB-S 170	Binder GmbH, Germany
Laminar Air Flow Bench	Scanlaf Mars	Labogene, Denmark
Microscope	Axiovert 25	Carl Zeiss, Germany
Multimode-Microplate Reader	Mithras² LB 943	Berthold Technologies, Germany
pH-meter	EC-30 pH	Phoenix Instruments, Germany
Shaker	RS-RS-5	Phoenix Instrument, Germany
Shaker/Agitator	Titramax 1000	Heidolph Instruments, Germany

3.1.2 Consumables

Table II. List of consumables

Equipment	Manufacturer
Blotting pads	VWR International GmbH, Darmstadt
Cell culture disposable plastic ware (flask, plates, tubes, serological pipettes and tips)	Sarstedt, Germany
10 / 200 / 1000 µl filter tips refill	Starlab, UK
10 / 200 / 1000 µl Tip One® tips	Starlab, UK
Mini PROTEAN glass plates	Bio-Rad Laboratories GmbH, Feldkirchen
Mini PROTEAN short plates	Bio-Rad Laboratories GmbH, Feldkirchen
PVDF membrane (Immobilon FL Transfer Membran)	Sigma-Aldrich, Taufkirchen

3.1.3 Chemicals and reagents

Table III. List of chemicals/reagents

Chemicals / reagents	Manufacturer
Ammonium persulfate (APS)	Sigma-Aldrich, Germany
Bovine serum albumine (BSA)	Sigma-Aldrich, Germany
EveryBlot Blocking Buffer	BioRad, Germany
ECL-reagent Western-Clarity	Sigma-Aldrich, Germany
DL-Dithiothreitol	Carl Roth GmbH & Co KG, Germany
Glycin	Carl Roth GmbH & Co KG, Germany
Human serum albumin	Sigma-Aldrich, Germany
Skimmed milk powder	Carl Roth GmbH & Co KG, Germany
4x Laemmli Sample Buffer	BioRad, Germany
Protease/Phosphatase Inhibitor Cocktail 100x	Cell Signaling, Germany
TEMED	Carl Roth GmbH & Co KG, Germany
TBS 1% Casein Blocker	BioRad, Germany
Tris Base	Carl Roth GmbH & Co KG, Germany
Pierce BCA Protein Assay Kit	Thermo Scientific, Germany
ECL-reagent Western-Ready Substrate Kit	PAN Biotech, Germany

3.1.4 Media and buffer

Table IV. List of media/buffer

Product	Manufacturer
Dulbecco´s Modified Eagle Medium (DMEM)	Pan Biotech, Germany
RPMI Medium 1640 (1x)	Thermo Fisher Scientific, UK
Selection Medium	Thermo Fisher Scientific, UK
Zeocin Medium	Thermo Fisher Scientific, UK
OptiMEM (1x) + GlutaMAX™-I Reduced Serum Medium	Thermo Fisher Scientific, UK
Transfection Medium	Thermo Fisher Scientific, UK
TrypLE™ Express	Thermo Fisher Scientific, Denmark
DPBS (Dulbecco´s Phosphatase Buffered Saline)	PAN Biotech, Germany

3.1.5 Primary and Secondary Antibodies used for Western blot analysis

Table V. List of primary/secondary antibodies

Antibody	Host	Company	Order no.	Dilution	Incubation Conditions
MyD88 (E-11)	Mouse	Santa Cruz Biotechnology	74532	1:1000	Overnight 4ºC
TICAM-1 (E-7)	Mouse	Santa Cruz Biotechnology	514384	1:1000	Overnight 4ºC
Anti-mouse IgG, HRP-linked Antibody, 1.0 ml	Mouse	Cell signaling	7076	1:2000 in 5% nonfat dried milk in TBS-T	1h RT

3.1.6 Software

Table VI. List of software

Software	Version	Developer
BioRender	-	SaaS, Toronto, Canada
ImageLab	6.1	Bio-Rad Laboratories, Germany
Prism 8.0	8.0.1	GraphPad, USA
MicroWin	8.34	Labsis Laborsysteme GmbH, Germany
Microsoft Office	Student	Microsoft Corporation, USA

3.2 Methods

3.2.1 Cell culture

In our work we have used the following cell lines: HEK293 cells, HEK-Blue cells, HaCaT cells and THP-1 monocytes.

HEK293 cells are immortalised cells derived from primary human embryonic kidney cells. They are frequently used to produce therapeutic proteins and viruses for gene therapy. These cells retain an epithelial-like morphology and adhere to the culture surface. Typically, they exhibit a pyramidal shape and display filopodia on their surface (47).

HEK-Blue cells are a stable clone expressing the secreted embryonic alkaline phosphatase (SEAP) reporter gene, regulated by the IFN-beta minimal promoter fused with five NF-kB and AP-1 binding sites. Activation of NF-kB leads to increased SEAP expression, which can be easily detected in the cell medium using the Quanti-Blue reagent, as SEAP is secreted (48). HEK-Blue hTLR2 KO-TLR1/6 cells are designed to study TLR2 signaling pathways, serving as control for HEK-Blue hTLR2-TLR6 cell line. In these KO cells, the endogenous TLR1 and TLR6 genes are knocked out, while human TLR2 and CD14 genes are stably transfected (49).

HaCaT cells are immortalised human keratinocytes and have been extensively used to study the epidermal homeostasis and its pathophysiology. This cell line is a non tumorigenic monoclonal cell line, adapted to long term growth without feed-layer or supplemented growth factors (50,51). It exhibits normal morphogenesis and expresses all the major surface markers and functional activities of isolated keratinocytes. They can also form stratified epidermal structure, but they can revert, back and forth, between a differentiated and a basal state upon changes in Ca^{2+} concentration in the medium (50–53).

THP-1 (Tohoku Hospital Pediatrics-1) is a human leukaemia monocytic cell line, derived from the peripheral blood of a childhood case of acute monocytic leukaemia (M5 subtype). THP-1 cells, including their genetically engineered derivatives, represent valuable tools for investigating monocyte structure and function in both health and disease. It has been extensively used to study monocyte/macrophage functions, mechanisms, signaling pathways and drug transport (54).

HEK Blue hTLR2-hTLR1, hTLR2-hTLR6, TLR2KO-TLR1/6, hTLR4, Null1 and Null2 cells were obtained from InvivoGen and were cultured in DMEM medium supplemented with 10% fetal bovine serum (FBS), 2mM L-glutamine, 100 U/mL penicillin, 100 µg/mL streptomycin, 100 µg/mL normocin and selective antibiotics. For the HEK Blue cells the selection antibiotic was added to the medium, and for HEK-Blue Null1 and Null2 cells the medium was supplemented with 100 µg/mL of zeocin.

HEK-293 cells were cultured in high glucose supplemented with 10% FCS, 2mM L-glutamine, 100 U/mL penicillin and 100 µg/mL streptomycin. The HaCaT cells were cultured in RPMI 1640 supplemented with 10% FCS, 2mM L-glutamine, 100 U/mL penicillin and 100 µg/mL streptomycin and were grown until 80% confluency was reached. THP-1 cells were cultured in RPMI 1640 medium supplemented with 10% FBS, 100 U/mL penicillin, 100 µg/mL streptomycin, 2 mM L-glutamine, and 0.05 mM 2-mercaptoethanol.

3.2.2 Defreezing, seeding and passaging the cells

Cell cultures can be maintained for many years if they are preserved in liquid nitrogen through cryopreservation, using a cytoprotective agent that is added to complete medium, such as dimethyl sulfoxide (DMSO), that allows the slow freezing of cells and prevents the formation of water crystals that could rupture the cell membranes (55).

Cells stored in liquid nitrogen were thawed by being resuspend in 5 mL of gently warmed culture medium and afterwards the cells were centrifuged for 5 minutes at 200 x *g* at room temperature. The supernatant was discarded, and the cell pellet was resuspended in complete medium and seeded into a new cell culture flask. Cells were grown at 37°C, with CO_2 content of 5% and a relative humidity of 96%.

The seeding and stimulation experiments were carried out under aseptic conditions in a laminar airflow bench. All equipment was either autoclaved or disinfected with 70% isopropanol before use, or disposable equipment was utilized. The cell cultures were maintained in T-25 or T-75 flasks within an incubator set at 37 °C with 5% CO_2.

When cells reached 80% of confluency, the medium was discarded, and cells were washed with Dulbecco's phosphate-buffered saline (DPBS). For the HaCaT cells the DPBS was aspirated and then the trypleExpress was added. Cells were briefly incubated at 37ºC to favour cell detachment. Afterwards, the cells were counted and centrifuged for 5 minutes at 200 x *g*, at room temperature. The supernatant was discarded, and the cells were resuspended in fresh medium and plated at the desired concentration.

Cells were counted with the help of a Luna-FL II automated cell counter. When cells were over 20–25 passages or if any abnormal growth or morphology was detected, they were discarded, and a new cell vial was thawed.

3.3 Protein Detection by Western Blot

Western Blot is a technique that allows the identification and quantification of specific proteins and is used to detect the expression levels of the proteins of interest as well as to study protein-

protein interactions. This method relies on the specific interaction of antibodies with target antigens present in the sample mixture (56).

3.3.1 Preparation of cell lysates

Cell lysis is a critical step in isolating intracellular proteins, nucleic acids, and other biomolecules for downstream applications such as Western blotting, PCR, or enzymatic assays. This process disrupts the cell membrane and releases cellular contents into a lysate, which can then be further analysed or processed (57).

HEK blue TLR4, HEK TLR2/1, HEK TLR2/6, HaCaT, THP-1 monocytes and HEK 293 cells were cultured in the respective medium. Once the cells reached 80–90% confluence, they were washed with cold PBS to remove any remaining culture medium. The lysis buffer (RIPA-buffer) was freshly prepared consisting of 1M Tris-HCl (pH 7.4), IGEPAL (NP-40), sodium deoxycholate (10%), 5M NaCl, 1 mM EDTA, and a protease inhibitor cocktail 100x (added just before use). The cells lysates were incubated on ice for 30 minutes under agitation, then the cell suspension was transferred to a microtube. Afterwards, the suspension was centrifuged at 18500 × *g* for 30 minutes at 4°C to remove cell detritus. The supernatant containing the soluble protein fraction was collected, aliquoted, and stored at -80°C for subsequent analysis.

3.3.2 Protein quantification in cell lysates

In this study, the BCA assay was selected for protein quantification due to its compatibility with common reagents in cell lysates and its high sensitivity, allowing for the detection of low protein concentrations (58).

According to the protocol Pierce BCA Protein Assay (Thermo Scientific), a standard curve was prepared using dilutions of bovine serum albumin (BSA) from 0 to 2000 µg/mL. In each quantification the correlation coefficient of the calibration line was higher than 0.99 and the estimation of protein levels in the quality controls samples did not diverge more than ± 5%.

Cell lysates were diluted in 1:5 ratio in RIPA buffer. Following the manufacturer's protocol, 25 µL of each BSA standard and diluted cell lysates were transferred to a 96-well microplate. Subsequently, 200 µL of BCA reagent was added to each well and the plate was incubated at 37°C for 30 minutes to facilitate colour development and then cooled down for 30 minutes at room temperature. Afterwards, the absorbance was measured on a plate reader at 560 nm. Absorbance readings were recorded, and protein concentrations in the cell lysates were determined by interpolating the values from the standard curve using a linear regression analysis. All samples were analysed in duplicate to ensure reliability and reproducibility of the results.

3.3.3 Preparation of samples and SDS-polyacrylamide gels

The loading buffer was prepared by mixing 4x Laemmli sample buffer (Bio-Rad) and 40x DTT solution (Sigma) in a 10:1 ratio. Protein samples were diluted as necessary to achieve the desired concentration of 20–40 µg per lane. Following the addition of the loading buffer, samples were denatured by heating for 5 minutes at 100ºC and cooling down on ice. Afterwards, the samples were centrifuged for 5 minutes at 18500 x *g*, at 4ºC and stored in the freezer at -80ºC.

In this study, SDS-PAGE was employed to analyse the protein composition of cell lysates and assess differences in protein expression under various experimental conditions. To simplify and standardize polyacrylamide gel preparation, the TGX Stain-Free FastCast Acrylamide Kit, 10% (Bio-Rad, Hercules, CA, USA) was utilized. The gel casting procedure was carried out according to the manufacturer's instructions. Equal volumes of Solution A (acrylamide/bis-acrylamide solution) and Solution B (tris-Glycine buffer) were mixed to form a 10% running gel, followed by the addition of 50 µL of 10% ammonium persulfate (APS) and 5 µL of TEMED to initiate polymerization. The solution was then poured between the glass plates of the gel allowed to polymerize at room temperature for approximately 30 minutes. After polymerization, a stacking gel was prepared using the same kit, following the manufacturer's guidelines for the lower acrylamide concentration.

Once the gels were polymerized, the gel assembly was placed in an electrophoresis chamber filled with running buffer (24.9 mM Tris, 191.8 mM glycine, 0.1% SDS). Protein samples (25 µg of total protein), prepared as described earlier, were loaded into the wells along with a molecular marker for size estimation. Electrophoresis was conducted at a constant voltage of 150 V for approximately 20 minutes, until the molecular marker started to expand in the running gel and then at 250 V for 20 minutes, until the dye front reached the bottom of the gel.

The stained gels were activated using a UV imager (Bio-Rad ChemiDoc) immediately after electrophoresis.

3.3.4 Protein Transfer

After electrophoresis, proteins were transferred from the polyacrylamide gel to a polyvinylidene fluoride (PVDF) membrane using a semi-dry transfer method. The gel was first equilibrated in transfer buffer (25 mM Tris, 191.8 mM glycine) for approximately 15 minutes to ensure proper protein binding to the membrane.

Prior to use, the PVDF membranes were activated by soaking in 20% (v/v) methanol for approximately 20 seconds, then in dH_2O for 2 minutes and in transfer buffer for 10 minutes.

The transfer setup was assembled in a specific order to create a “sandwich” structure. Afterwards, the transfer was conducted using the standard protocol of the BioRad TransBlot Turbo System. The semi-dry transfer was performed at a constant voltage of 15V for 30 minutes. This allowed proteins to migrate from the gel into the membrane via an electric field.

Following the transfer, the membrane was imaged to check the efficiency of the transfer. After imaging, the membrane was washed with deionized water to remove the stain, preparing it for subsequent blocking and antibody incubation steps.

3.3.5 Membrane Blocking and Antibody Incubations

To minimize non-specific background interactions during antibody detection, the membrane was blocked using a blocking buffer. The blocking buffer was prepared consisting of 5% (w/v) non-fat dry milk dissolved in TBS-T (Tris-buffered saline with 0.1%Tween 20). The membrane was incubated in this blocking buffer for 1 hour at room temperature under gentle agitation.

Following the blocking step, the membrane was rinsed briefly with TBS-T to remove any unbound blocking agent. The primary antibody, MyD88 (E-11), was then diluted according to the manufacturer´s instructions and applied to the membrane, ensuring complete coverage. This incubation was performed overnight at 4°C, under gentle agitation.

After incubating with the primary antibody, the membrane was washed three times with TBS-T to remove non-specifically bound antibodies. Subsequently, the membrane was incubated with a secondary antibody conjugated to a detection enzyme, specifically horseradish peroxidase (HRP). The secondary antibody, anti-mouse IgG, was diluted in the appropriate buffer, similarly to the primary antibody, and the incubation was carried out for 1 hour at room temperature, under gentle agitation.

In addition to the MyD88 primary antibody, the same membrane was used for subsequent detection of TICAM-1/TRIF (E-7) protein levels. This primary antibody was also incubated overnight at 4ºC with gentle agitation. The following day, the membrane was washed again with TBS-T before being incubated for one hour with an HRP-conjugated secondary antibody (anti-mouse IgG). The secondary antibody was diluted in blocking buffer with a specific dilution ratio, ensuring optimal detection of the TICAM-1 protein. Afterwards, the membrane was washed three times for five minutes in TBS-T.

3.3.6 Detection of proteins

Protein bands were detected using enhanced chemiluminescence reagents from the Western-Ready ECL substrate Kit (BioLegend). Following the incubation of the membrane with the

chemiluminescent substrate, the bands were visualized using the ImageQuant LAS 4000 mini chemiluminescence imaging analysis system (GE Healthcare Life Sciences, PA, USA).

3.4. Quanti Blue Assay

QUANTI-Blue™ is a colorimetric enzyme assay used to determine any alkaline phosphatase activity (AP) in a biological sample, such as supernatants of cell cultures. QUANTI-Blue™ Solution changes from a pink to a purple-blue colour in the presence of AP. This method is highly sensitive for quantitative measurement and can determine secreted AP activity without disturbing cells, thus allowing the repeated sampling of cell cultures for kinetic studies (59).

Two ligands were used to stimulate the cells: HKEB and HKSA. HKEB is a heat killed preparation of the Gram-negative bacterium, *E.coli O111:B4* that contain cell wall components, such as peptidoglycan (PGN) and lipopolysaccharide (LPS), recognized by TLR2 and TLR4. Additionally, HKSA is a lyophilized heat-killed preparation of *Staphylococcus aureus*, a Gram-positive extra-cellular growing bacterium that is mainly recognized by TLR2. In this experiment, HEK-Blue Null cells lacking hTLR2 and hTLR4 and TLR2 KO-TLR1/6 cells served as control.

3.4.1 Stimulation of HEK-Blue cells with TLR ligands

HEK-Blue cells were plated at a density of 40.000 cells/well, in 96-well plates, and let to grow for 48 hours, or 24 hours, in case of the control cells. Cell medium was replaced, and the cells were then stimulated with increasing concentrations of HKEB and HKSA. The stock vials contained $1x10^{10}$ freeze-dried cells, and from this stock serial dilutions of HKEB and HKSA were prepared, to stimulate HEK-Blue cells: $1000x10^6$, $100x10^6$, $20x10^6$, $10x10^6$, $1x10^6$, $0,1x10^6$ and $0,01x10^6$ cells/mL of HKEB, and $1000x10^6$, $100x10^6$, $10x10^6$ $1x10^6$, $0,1x10^6$, $0,01x10^6$, and $0,001x10^6$ cells/mL of HKSA.

Control cells HEK-Blue TLR2 KO-TLR1/6, Null1 and Null2, were stimulated with the unique concentration of $100x10^6$ of both HKSA and HKEB. Finally, the plates were incubated for 24h at 37ºC.

3.4.2 Quantification of SEAP in cultured medium

Quanti Blue substrate was prepared following manufacturer instructions, and 20 µL of the medium of each sample was added to 180 µL of the substrate that had been previously dispensed in the wells of a 96 well plate. Immediately after, the plate was measured in a plate reader at 620 nm ±10 nm as an excitation filter. In total, 5 measurements were made of the same plate with a 5-minute interval. The same experiment was performed independently for three times.

3.5 ELISA Assay

ELISA is based on the concept of antigen–antibody reactions, representing the chemical interaction between antibodies produced by the B cells of leukocytes and antigens. It permits the highly sensitive and selective quantitative/qualitative analysis of antigens, including proteins, peptides, nucleic acids and hormones (60).

3.5.1 Seeding and stimulation of HaCaT cells

HaCaT cells were cultured evenly in 24-well plate at a density of $0,1x10^6$ cells/well and after 24h cells were stimulated with the previous indicated concentrations of HKEB and HKSA. The old medium was aspirated and 1 mL of PBS was added into each well. Afterwards, the PBS was aspirated and 500 µl of cell medium or the HKEB or HKSA dilutions that were made were added in each respective well. The plate was incubated at 37ºC for 24 hours and after that the supernatant of each well was transferred to a 1,5 mL microtube and stored at -80ºC until the measurement was done.

Finaly, concentrations of IL-8 cytokines in the supernatants were detected using ELISA kit (ELISA-Ready Set Go; Invitrogen by Thermo Fisher Scientific, Darmstadt, Germany) according to its instruction. The absorbance was read at 450 nm using a microplate reader (Thermo Fisher Scientific, United States). The same experiment was performed independently two times.

4.Results

4.1 MyD88 and TICAM-1 show a distinct expression profile in various cell lines

As previously mentioned, MyD88 and TRIF pathways are the two branches activated downstream of TLR4, while in the case of TLR2 the MyD88-dependent pathways is the one preferentially activated. Activation of the MyD88 pathway induces the expression of a variety of MyD88 dependent inflammatory cytokines such as TNF-α, IL-6, IL-12A, and IL-12B, while activation of the TRIF pathway induces the expression of TRIF dependent cytokines such as IL-10 (9,28,29). To analyse the expression patterns of MyD88 and TRIF in the cell lines used in our study, such as HEK Blue hTLR4, HEK Blue hTLR2-hTLR1, HEK Blue hTLR2-hTLR6, and HaCaT, as well as THP-1 monocytes and HEK293 cells, the MyD88 and TICAM-1 (TRIF) protein levels were determined by Western Blot (**Figure 3A and 3B**).

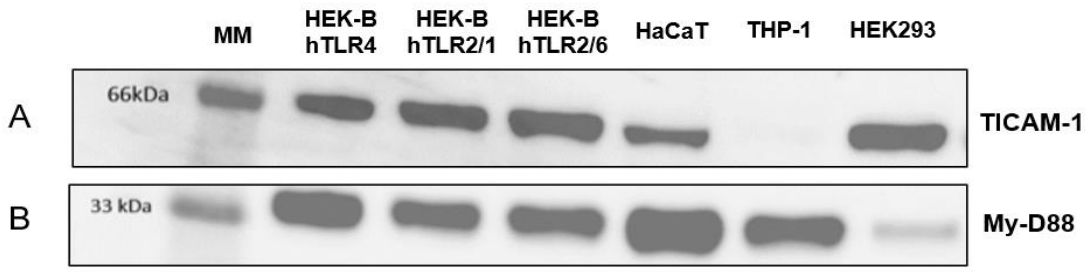

Figure 3. Protein expression levels of TICAM-1 and MyD88 in various cell lines.

Western blot analysis of the expression levels of **(A)** TICAM-1 and **(B)** MY-D88 in HEK Blue hTLR4, hTLR2-hTLR1 and hTLR2-hTLR6, HaCaT cells, THP-1 monocytes and HEK293 cells.

Protein expression levels showed that both HEK Blue and HEK293 cell lines express high levels of TRIF when compared with HaCaT cells. Interestingly, in THP-1 monocytes no expression was detected **(Figure 3A).**

While HaCaT cells expressed lower TRIF levels, MyD88 expression was higher in this cell line. HEK Blue reporter cell lines and THP-1 monocytes also expressed high levels of MyD88. Interestingly, the HEK293 parental cell line expressed lower MyD88 levels compared to the HEK Blue cell line, suggesting that TLR overexpression engineered in HEK-blue cells may increase MY-D88 levels **(Figure 3B).**

4.2 Heat-killed bacteria preferably activate TLR2 heterodimers depending on the bacterial species

Understanding the modulation of TLR by specific agonists and the downstream activation of TLR-dependent signaling is crucial for deciphering the immune response mechanisms (61). To gain new insights into the mechanism underlying TLR protein agonists, a dose−response analysis in HEK-blue reporter cells expressing either human TLR4 (hTLR4), human TLR2/1 or human TLR2/6, stimulated by either HKEB or HKSA was performed. As previously mentioned, HEK-Blue cells are a stable clone expressing SEAP reporter gene under the control of the IFN-beta minimal promoter fused with five NF-kB and AP-1 binding sites, so the activation of the NF-kB results in an increase in SEAP expression (48).

The EC_{50} (half maximal effective concentration) refers to the concentration of any bioactive compound, which induces a response halfway between the baseline and maximum after a specified exposure time (62). In the dose–response curve of the two bacteria's cell extracts, HKEB and HKSA, a significant difference was observed in EC_{50} values.

In HEK hTLR2-hTLR6 cells, that specifically express both TLR2 and TLR6, a lower EC_{50} value for HKSA (EC_{50}=2.56 cells/mL) indicates that it is more potent than HKEB (EC_{50}=17.39

cells/mL), as it produces the same desired effect at a lower dose. However, similar maximum effect, or E_{max} value, was obtained for both cell extracts (HKEB Emax = 0.99 OD_{620nm} and HKSA Emax = 1.21 OD_{620nm}) **(Figure 4A).**

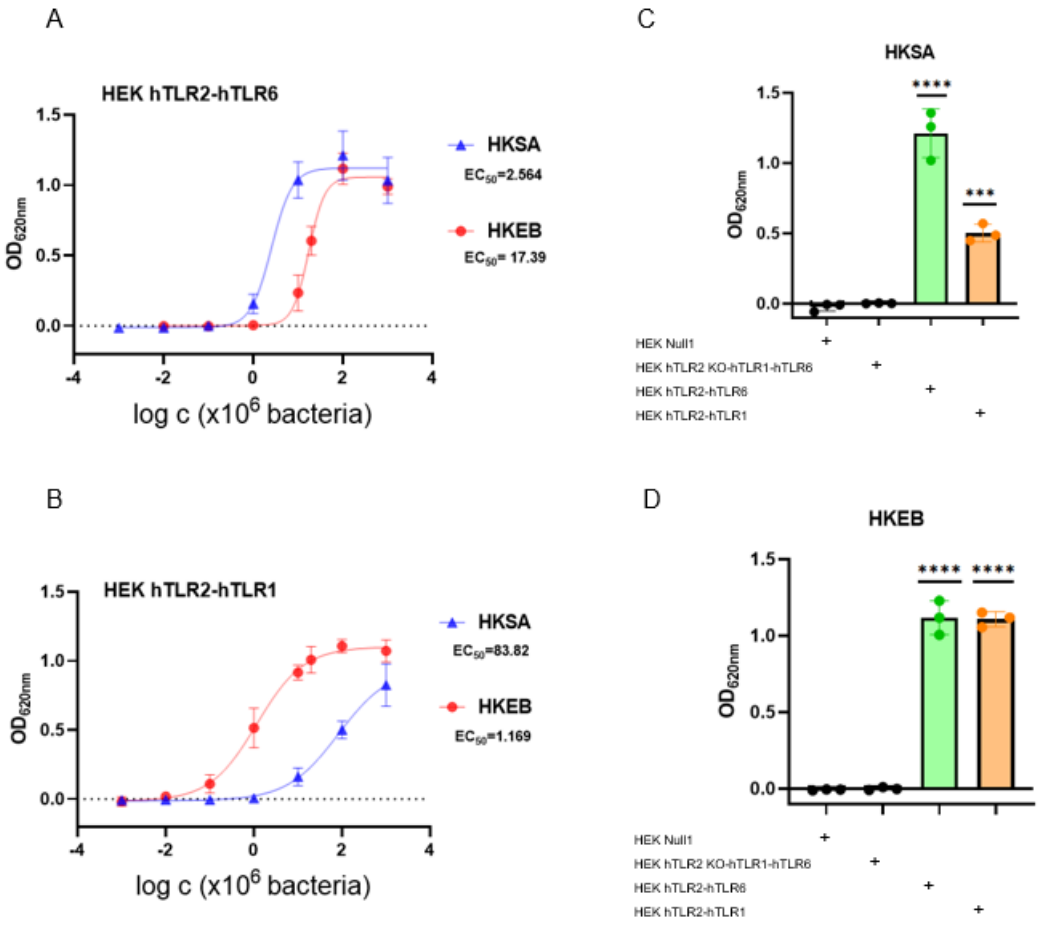

Figure 4. Activation of TLR2 in HEK-Blue cells by HKSA and HKEB.

HEK-Blue hTLR2-TLR6, HEK-Blue hTLR2-TLR1, HEK Null1 and HEK-Blue hTLR2 KO-TLR1/6 cells were incubated with increasing concentration of HKEB (heat killed *E. coli*; Gram- bacteria) and HKSA (heat killed *S. aureus*; Gram+ bacteria). After 24h, SEAP reporter levels were determined by reading the optical density (OD) at 620 nm. **(A)** Dose-response curve of hTLR2-TLR6 treated with HKEB (red) and HKSA (blue). **(B)** Dose-response curve of hTLR2-TLR1 treated with HKEB (red) and HKSA (blue). **(C,D)** Comparison the activity of different cells in response to HKSA and HKEB, respectively. Error bars represent SD from triplicate samples (n=3). Statistical significance was determined using one-way ANOVA analysis with a Turkey-Krammer Post-Test, with significance levels indicated by ***P < 0.001; ****P < 0.0001.

Interestingly, in HEK hTLR2-hTLR1 cells, that specifically express TLR2 and TLR1, a lower EC_{50} value was obtained for HKEB (EC_{50} =1.17 cells/mL) when comparing the EC_{50} value for HKSA (EC_{50} =83.82 cells/mL), which indicates that HKEB is more potent than HKSA, as it produces the same desired effect at a lower dose. Moreover, there is also a slight difference in the maximum effect, or E_{max} values obtained, since the E_{max} value for HKEB was 1.11

OD_{620nm} and for HKSA was 0.83 OD_{620nm}. Therefore, the treatment with HKSA, at the tested concentrations, did not activate the IFN-beta minimal promoter to the same extent **(Figure 4B).**

Comparing the control cells (HEK Null 1 cells and HEK-Blue hTLR2 KO-TLR1/6 cells) with HEK-Blue hTLR2-TLR1 and HEK-Blue hTLR2-TLR6 respectively, we firstly observe that TLR2 heterodimerization is indispensable to convey the activation of the receptor by either HKSA or HKEB **(Figure 4C and 4D).** Therefore, treatment with HKSA led to a higher response in the cell lines that express TLR2 and TLR6, when compared with HEK-Blue hTLR2-TLR1 cells, since the higher activity obtained in HEK-Blue TLR2/6 was 1.21 OD_{620nm} and in HEK-Blue TLR 2/1 was 0.50 OD_{620nm} (**Figure 4C).** Furthermore, HKEB induced a similar response in both hTLR2-TLR1 and hTLR2-TLR6 cells since the higher activity obtained for HEK-Blue TLR2/6 was 1,12 OD_{620nm} and in HEK-Blue TLR 2/1 was 1.11 OD_{620nm} **(Figure 4D).**

Next, a dose−response analysis in HEK-blue reporter cells expressing human TLR4 was performed because hTLR4 is well-characterized in existing literature (63), so this allowed us to ensure that our methodology was reliable after analysing the activation of hTLR2/1 and hTLR2/6.

In HEK blue hTLR4 that stably express TLR4, we observed that HKEB activated the TLR4-dependent NF-κB response with an EC_{50}=10.94 cells/mL. Interestingly, TLR4 was not activated by HKSA (EC_{50}=204.5 cells/mL) **(Figure 5A).**

The analysis of HEK cells lacking TLR4 (HEK Null2) showed no NF-κB activation after stimulation with HKEB (OD_{620nm}=0) or HKSA (OD_{620nm}=0.01), respectively. Comparing the control cells with HEK cells expressing TLR4, a significant response induced by HKEB treatment in HEK-hTLR4 cells (OD_{620nm}= 0.94, ***p < 0.001) **(Figure 5B)**, but not by HKSA (OD_{620nm}= 0.01; P-value not significant) was observed **(Figure 5C).**

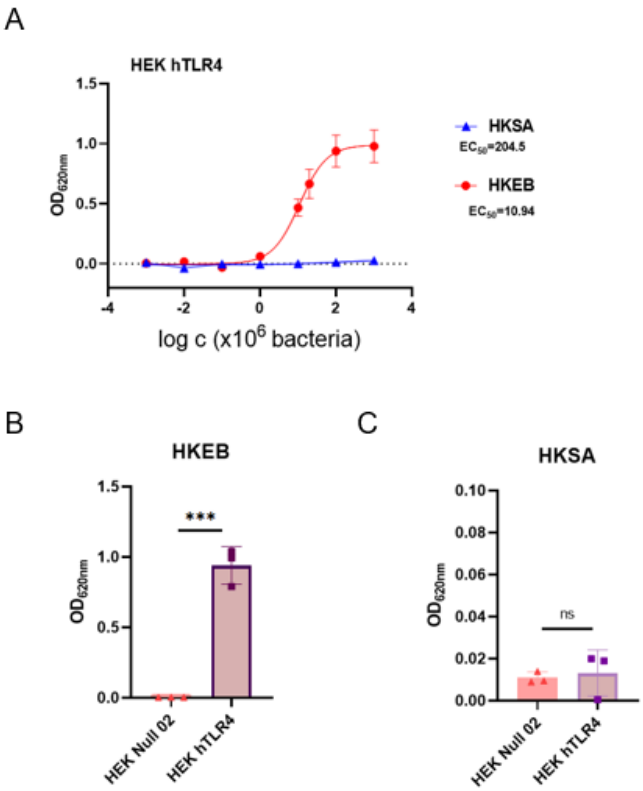

Figure 5. Activation of TLR4 in HEK-Blue cells by heat-killed bacteria.

HEK-Blue hTLR4 and HEK Null2 were incubated with increasing concentration HKEB (heat killed *E. coli*; Gram- bacteria) and HKSA (heat killed *S. aureus*; Gram+ bacteria). After 24h, SEAP reporter levels were determined by reading the optical density (OD) at 620 nm. (**A)** Dose-response curve of HEK hTLR4 cells treated with heat-killed *E. coli* (HKEB, red) and *S. aureus* (HKSA, blue). **(B)** Comparison of HEK hTLR4 and HEK Null2 cells in response to HKEB. HEK hTLR4 cells show significant activation (***p < 0.001). **(C)** Comparison of HEK hTLR4 and HEK Null2 cells in response to HKSA, showing no significant difference (ns, not significant). Error bars represent SD from triplicate samples (n=3). Statistical significance was determined using Student´s t-test, with significance levels indicated by ***p < 0.001.

4.3 High concentrations of heat-killed bacteria lead to IL-8 release in HaCaT cells

Since functional TLRs induce a biological response, IL-8 expression levels were examined in the supernatant of HaCaT cells, after stimulation with different doses of the TLR ligands (HKSA and HKEB) using an ELISA.

At higher concentrations, HKEB and HKSA treatment led to a dose-dependent secretion of IL-8. Indeed, at lower bacterial concentrations (below log 2), IL-8 levels were undetectable after both treatments. However, as the concentration of HKEB and HKSA increased beyond 10^2 bacteria, IL-8 secretion increased concomitantly, reaching levels around 2943.58 pg/mL (mean ± SD, n=2) and 7007 pg/mL (mean ± SD, n=2), respectively **(Figure 6A e 6B).** Interestingly, IL-8 secretion in response to HKSA appears higher than for HKEB, particularly at the highest concentration.

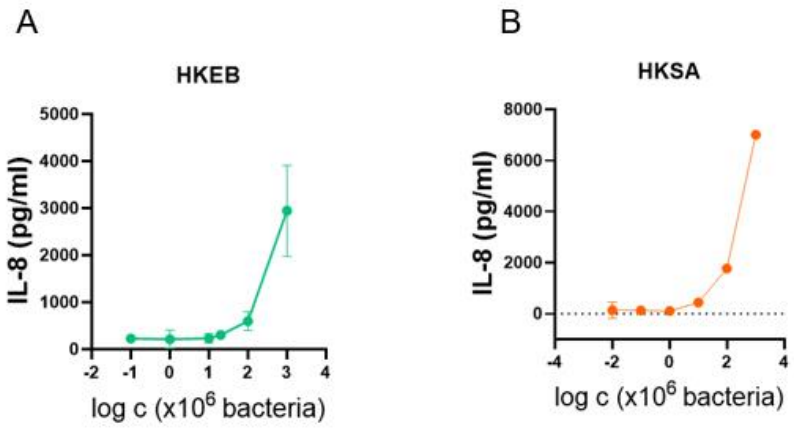

Figure 6. IL-8 secretion from HaCaT cells.

HaCaT cells were cultured and stimulated with increasing concentrations of **(A)** HKEB (heat killed *E. coli*; Gram- bacteria) and **(B)** HKSA (heat killed *S. aureus*; Gram+ bacteria). IL-8 was detected by ELISA in the 24-hour supernatant following stimulation. A dose-response curve was made for both. Error bars represent SD from duplicate samples (n=2).

5. Discussion

To explore the mechanisms of TLR signaling in immune responses, the study was initiated with a Western blot analysis to assess the expression profiles of the key adaptor proteins TRIF and MYD88 across multiple cell lines. These lines included engineered HEK-Blue cells expressing specific TLRs, HaCaT keratinocytes, THP-1 monocytes, and HEK293 cells. Understanding how these proteins are expressed across different cellular contexts provided the basis for evaluating each cell line's capacity to respond to TLR-mediated immune signaling. In the Western blot analysis, it was observed that HEK-Blue cells, engineered to overexpress TLR4, TLR2/1, and TLR2/6, showed robust expression of TRIF, aligning with their role in TRIF-dependent signaling primarily mediated by TLR4. This high expression suggests that HEK-Blue cells are prepared for TLR-mediated immune activation, potentially enabling a rapid response to pathogens. Interestingly, HaCaT keratinocytes, epithelial cells essential in skin immunity, displayed weaker TRIF expression, reflecting their more localized immune role with a reduced dependence on the TRIF pathway (64,65). THP-1 monocytes, which play an essential role in pathogen recognition and inflammatory responses, did not express TRIF, suggesting their signaling relies more on MYD88, consistent with their typical MYD88-dependent signaling patterns in response to TLRs, especially TLR2 and TLR4 (66,67). Lastly, HEK293 cells, which are non-immune cells, surprisingly showed strong expression of TRIF, hinting at an underexplored potential for innate immune signaling in non-immune cells. These cells could also be a good model for compound testing regarding the TRIF dependent pathway since there are already some cells on the market, that have a reporter gene for the TRIF dependent signaling pathway (e.g. HEK-Dual™ hTLR4 Cells). HEK-Blue cells also demonstrated high MYD88 expression across all engineered lines, consistent with the central role MYD88 plays in mediating signaling for most TLRs, excluding TLR3. The high expression levels across these lines validate their design for TLR-dependent immune studies. In HaCaT cells, an unexpectedly high MYD88 expression was noted, potentially underscoring the readiness of keratinocytes to engage in MYD88-dependent responses during skin inflammation or infection (68,69). THP-1 monocytes, as expected, exhibited strong MYD88 expression, underscoring its central role in monocyte and macrophage immune function. By contrast, HEK293 cells exhibited only faint MYD88 expression, which aligns with their limited role in TLR-mediated signaling under non-inflammatory conditions (70).

After confirmation that the cell lines used express the necessary adaptors for TLR signaling, the aim was to characterize the TLR activation profile in response to specific agonists. HEK-Blue reporter cells were stimulated with heat-killed *Escherichia coli* (HKEB) and *Staphylococcus aureus* (HKSA), chosen as representative Gram-negative and Gram-positive bacteria, respectively. HEK-Blue cells, engineered to express subsets of TLR receptors

(TLR2/1, TLR2/6, and TLR4), provided a controlled setting to assess receptor-specific activation. Furthermore, HEK blue hTLR2/1 cells responded robustly to HKEB, while hTLR2/6 cells were more responsive to HKSA. Meanwhile, hTLR4 cells displayed strong activation in response to HKEB but no response to HKSA. These findings align with existing literature that TLR2/1 heterodimers primarily recognize *E. coli*-derived lipoproteins, while TLR2/6 recognizes similar structures in *S. aureus* (29,71). The activation of TLR4 by HKEB but not HKSA supports known data that HKEB is a TLR4 agonist, whereas HKSA does not strongly interact with TLR4 (72,73). This ligand-specific activation suggests that distinct TLRs may drive tailored immune responses based on pathogen type, a finding with potential implications for vaccine design.

Building on the activation profile of TLR receptors, cytokine responses were analysed, particularly IL-8 secretion, in HaCaT cells upon exposure to HKSA and HKEB. The aim was to understand how gram-positive and gram-negative bacterial components influence inflammatory cytokine production in keratinocytes. The analysis demonstrated a higher IL-8 response to HKSA than HKEB, particularly at higher bacterial concentrations, indicating that HaCaT cells may be more sensitive to gram-positive bacterial components (74) or that TLR2-mediated signaling drives a stronger IL-8 response compared to TLR4-mediated pathways. This observation aligns with our earlier finding that MYD88 expression is notably high in HaCaT cells, supporting the idea that TLR2 signaling through MYD88 may drive a more robust inflammatory response in skin cells. The IL-8 secretion patterns suggest a threshold concentration is needed to trigger significant TLR signaling, with lower bacterial loads insufficient to activate a strong response. However, once this threshold is reached, IL-8 secretion increases, underscoring the capacity of HaCaT cells to respond to varying bacterial loads. This dose-dependent IL-8 production provides insight into the inflammatory capacity of keratinocytes and their specific sensitivity to Gram-positive bacteria, which are frequent agents in skin infections (75,76). Given IL-8's role in recruiting neutrophils to infection sites, the strong response to *S. aureus* reflects the typical clinical association of Gram-positive bacteria with skin inflammation and infection, whereas *E. coli*, less frequently associated with skin infections, elicited a comparatively muted response (77,78).

These findings indicate that the selected *in vitro* models are effective for high-throughput screening of TLR ligands, providing a valuable tool for exploring TLR signaling specificity. This approach allows for efficient identification of specific TLR responses, which is essential for understanding the distinct functions of TLR pathways and their role in immune regulation. Future studies should integrate additional cell types to better replicate *in vivo* conditions and expand on the translational potential of these models.

6. Conclusion

The Western blot analysis confirmed that engineered HEK-Blue cells, with high TRIF and MYD88 expression, are ideal for studying TLR-mediated immune signaling. HaCaT keratinocytes and THP-1 monocytes show cell-type-specific reliance on MYD88, aligning with their localized and inflammatory roles, respectively. Interestingly, non-immune HEK293 cells exhibit TRIF expression, suggesting a potential, underexplored role in innate immunity. Overall, these expression profiles support the tailored use of these cell lines in TRIF- or MYD88-dependent TLR research.

Through TLR ligand stimulation, we confirmed that TLR2/1 and TLR2/6 heterodimers preferentially respond to HKEB and HKSA, respectively, corroborating findings in existing literature on TLR-ligand specificity. The absence of a TLR4 response to HKSA and its pronounced activation by HKEB further emphasizes the pathogen-specific nature of TLR signaling, which could be essential while designing immunotherapies. Additionally, the IL-8 secretion profiles in HaCaT cells revealed a stronger response to HKSA, highlighting the sensitivity of skin cells to Gram-positive bacteria, which are more frequently associated with skin infections. This IL-8 response, particularly the dose-dependent increase, aligns with the role of TLRs in pathogen-specific inflammatory responses.

Despite these findings, the study is limited by its reliance on the *in vitro* reporter models, which may not fully capture the complexity of *in vivo* immune responses or cytokine profiles. Further research could involve cytokine analysis *in vivo* and the finalized CRISPR/Cas9-mediated MYD88 knockout to elucidate MYD88's role in immune signaling. In fact, during our study, we also began to implement a CRISPR/Cas9 knockout of MYD88 in HEK293 cells to specifically examine MYD88's role in TLR signaling. The initial phases, including cell seeding and transfection, were completed, yet further steps, including clonal selection and knockout validation, remain for future studies. Completing this task could have helped to delineate MYD88's distinct contributions to immune responses, enhancing our understanding of TLR pathways and their manipulation for therapeutic purposes. Additionally, investigating other TLR-dependent pathways or alternative signaling molecules within these cells could provide a broader understanding of immune activation dynamics.

In summary, our findings contribute to a more detailed understanding of TLR-specific immune responses, reinforcing the value of receptor-specific targeting in therapeutic interventions. Expanding our understanding of the molecular pathways in TLR signaling could guide future research in developing more precise vaccines and immunotherapies designed for specific pathogens and targeted tissues.

7. References

1. Manuscript A. Overview of the immune response. Journal of Allergy and Clinical Immunology. 2010;125(2):S345.
2. Netea MG, Schlitzer A, Placek K, Joosten LAB, Schultze JL. Innate and Adaptive Immune Memory: an Evolutionary Continuum in the Host's Response to Pathogens. Cell Host Microbe. 2019;25(1):13–26.
3. Netea MG, Balkwill F, Chonchol M, Cominelli F, Marc Y, Giamarellos-bourboulis EJ, et al. A guiding map for inflammation. National Immunology. 2018;18(8):826–31.
4. Duan T, Du Y, Xing C, Wang HY, Wang RF. Toll-Like Receptor Signaling and Its Role in Cell-Mediated Immunity. Front Immunol. 2022;13(March):1–22.
5. Akira S, Uematsu S, Takeuchi O. Pathogen recognition and innate immunity. Cell. 2006;124(4):783–801.
6. Takeuchi O, Akira S. Pattern Recognition Receptors and Inflammation. Cell. 2010;140(6):805–20.
7. Cai X, Chiu YH, Chen ZJ. The cGAS-cGAMP-STING pathway of cytosolic DNA sensing and signaling. Mol Cell. 2014;54(2):289–96.
8. Hayden MS, Ghosh S. NF-κB in immunobiology. Cell Res. 2011;21(2):223–44.
9. Kawasaki T, Kawai T. Toll-like receptor signaling pathways. Front Immunol. 2014;5(SEP):1–8.
10. Arlaud GJ. Structural biology of C1. Biochem Soc Trans. 2002;30(5):A98–A98.
11. Kawai T, Akira S. The role of pattern-recognition receptors in innate immunity: Update on toll-like receptors. Nat Immunol. 2010;11(5):373–84.
12. Blasius AL, Beutler B. Intracellular Toll-like Receptors. Immunity. 2010;32(3):305–15.
13. Takemura N, Kawasaki T, Kunisawa J, Sato S, Lamichhane A, Kobiyama K, et al. Blockade of TLR3 protects mice from lethal radiation-induced gastrointestinal syndrome. Nat Commun. 2014;5.
14. Bernard JJ, Cowing-Zitron C, Nakatsuji T, Muehleisen B, Muto J, Borkowski AW, et al. Ultraviolet radiation damages self noncoding RNA and is detected by TLR3. Nat Med. 2012 Aug;18(8):1286–90.
15. Serrano Cardona L, Muñoz Mata E. Paraninfo Digital. Early Hum Dev. 2013;83(1):1–11.

16. Lee BL, Moon JE, Shu JH, Yuan L, Newman ZR, Schekman R, et al. UNC93B1 mediates differential trafficking of endosomal TLRs. Elife. 2013;2013(2):1–22.

17. Lee KG, Xu S, Kang ZH, Huo J, Huang M, Liu D, et al. Bruton's tyrosine kinase phosphorylates Toll-like receptor 3 to initiate antiviral response. Proc Natl Acad Sci U S A. 2012;109(15):5791–6.

18. Yamashita M, Chattopadhyay S, Fensterl V, Saikia P, Wetzel JL, Sen GC. Epidermal growth factor receptor is essential for toll-like receptor 3 signaling. Sci Signal. 2012;5(233):1–18.

19. Sameer AS, Nissar S. Toll-Like Receptors (TLRs): Structure, Functions, Signaling, and Role of Their Polymorphisms in Colorectal Cancer Susceptibility. Biomed Res Int. 2021;2021.

20. Kawai T, Akira S. Signaling to NF-κB by Toll-like receptors. Trends Mol Med. 2007;13(11):460–9.

21. Kobayashi K, Hernandez LD, Galán JE, Janeway CA, Medzhitov R, Flavell RA. IRAK-M is a negative regulator of Toll-like receptor signaling. Cell. 2002;110(2):191–202.

22. Chen F, Bhatia D, Chang Q, Castranova V. Finding NEMO by K63-linked polyubiquitin chain. Cell Death Differ. 2006;13(11):1835–8.

23. Sanjo H, Takeda K, Tsujimura T, Ninomiya-Tsuji J, Matsumoto K, Akira S. TAB2 Is Essential for Prevention of Apoptosis in Fetal Liver but Not for Interleukin-1 Signaling. Mol Cell Biol. 2003;23(4):1231–8.

24. Shim JH, Xiao C, Paschal AE, Bailey ST, Rao P, Hayden MS, et al. TAK1, but not TAB1 or TAB2, plays an essential role in multiple signaling pathways in vivo. Genes Dev. 2005;19(22):2668–81.

25. Li Q, Lu Q, Bottero V, Estepa G, Morrison L, Mercurio F, et al. Enhanced NF-κB activation and cellular function in macrophages lacking IκB kinase 1 (IKK1). Proc Natl Acad Sci U S A. 2005;102(35):12425–30.

26. Jiang X, Chen ZJ. The role of ubiquitylation in immune defence and pathogen evasion. Nat Rev Immunol. 2011 Dec;12(1):35–48.

27. Chang M, Jin W, Sun SC. Peli1 facilitates TRIF-dependent Toll-like receptor signaling and proinflammatory cytokine production. Nat Immunol. 2009 Oct;10(10):1089–95.

28. Brieger A, Rink L, Haase H. Differential Regulation of TLR-Dependent MyD88 and TRIF Signaling Pathways by Free Zinc Ions. The Journal of Immunology. 13 Aug 15;191(4):1808–17.

29. Oliveira-Nascimento L, Massari P, Wetzler LM. The role of TLR2 ininfection and immunity. Front Immunol. 2012;3(APR):1–17.

30. Colleselli K, Stierschneider A, Wiesner C. An Update on Toll-like Receptor 2, Its Function and Dimerization in Pro- and Anti-Inflammatory Processes. Int J Mol Sci. 2023;24(15):1–18.

31. Ozinsky A, Underhill DM, Fontenot JD, Hajjar AM, Smith KD, Wilson CB, et al. The repertoire for pattern recognition of pathogens by the innate immune system is defined by cooperation between Toll-like receptors. Proc Natl Acad Sci U S A. 2000;97(25):13766–71.

32. Su SB, Tao L, Deng ZP, Chen W, Qin SY, Jiang HX. TLR10: Insights, controversies and potential utility as a therapeutic target. Scand J Immunol. 2021;93(4):1–15.

33. Van Bergenhenegouwen J, Plantinga TS, Joosten LAB, Netea MG, Folkerts G, Kraneveld AD, et al. TLR2 & Co: a critical analysis of the complex interactions between TLR2 and coreceptors. J Leukoc Biol. 2013;94(5):885–902.

34. Kang JY, Nan X, Jin MS, Youn SJ, Ryu YH, Mah S, et al. Recognition of Lipopeptide Patterns by Toll-like Receptor 2-Toll-like Receptor 6 Heterodimer. Immunity. 2009;31(6):873–84.

35. Jin MS, Kim SE, Heo JY, Lee ME, Kim HM, Paik SG, et al. Crystal Structure of the TLR1-TLR2 Heterodimer Induced by Binding of a Tri-Acylated Lipopeptide. Cell. 2007;130(6):1071–82.

36. Lee SJ, Shin SJ, Lee SJ, Lee MH, Kang TH, Noh KT, et al. Mycobacterium abscessus MAB2560 induces maturation of dendritic cells via toll-like receptor 4 and drives th1 immune response. BMB Rep. 2014;47(9):512–7.

37. Long EM, Millen B, Kubes P, Robbins SM. Lipoteichoic acid induces unique inflammatory responses when compared to other toll-like receptor 2 ligands. PLoS One. 2009;4(5).

38. Manukyan M, Triantafilou K, Triantafilou M, Mackie A, Nilsen N, Espevik T, et al. Binding of lipopeptide to CD14 induces physical proximity of CD14, TLR2 and TLR1. Eur J Immunol. 2005;35(3):911–21.

39. Zheng H, Tan Z, Zhou T, Zhu F, Ding Y, Liu T, et al. The TLR2 is activated by sporozoites and suppresses intrahepatic rodent malaria parasite development. Sci Rep. 2015;5(September):1–10.

40. Oosenbrug T, van de Graaff MJ, Ressing ME, van Kasteren SI. Chemical Tools for Studying TLR Signaling Dynamics. Cell Chem Biol. 2017;24(7):801–12.

41. Kurkjian CJ, Guo H, Montgomery ND, Cheng N, Yuan H, Merrill JR, et al. The Toll–Like Receptor 2/6 Agonist, FSL–1 Lipopeptide, Therapeutically Mitigates Acute Radiation Syndrome. Sci Rep. 2017;7(1):1–13.

42. Funderburg N, Lederman MM, Feng Z, Drage MG, Jadlowsky J, Harding C V., et al. Human β-defensin-3 activates professional antigen-presenting cells via Toll-like receptors 1 and 2. Proc Natl Acad Sci U S A. 2007;104(47):18631–5.

43. Scheibner KA, Lutz MA, Boodoo S, Fenton MJ, Powell JD, Horton MR. Hyaluronan Fragments Act as an Endogenous Danger Signal by Engaging TLR2. The Journal of Immunology. 2006;177(2):1272–81.

44. Marks KE, Cho K, Stickling C, Reynolds JM. Toll-like receptor 2 in autoimmune inflammation. Immune Netw. 2021;21(3):1–13.

45. Rajpoot S, Wary KK, Ibbott R, Liu D, Saqib U, Thurston TLM, et al. TIRAP in the Mechanism of Inflammation. Front Immunol. 2021;12(July):1–12.

46. Lawson DH, Lee S, Zhao F, Tarhini AA, Margolin KA, Ernstoff MS, et al. This is to certify that. Journal of Clinical Oncology. 2016;1(1):97680.

47. Tan E, Chin CSH, Lim ZFS, Ng SK. HEK293 Cell Line as a Platform to Produce Recombinant Proteins and Viral Vectors. Front Bioeng Biotechnol. 2021;9(December):1–9.

48. Hu Z, Zhang T, Jiang S, Yin H. Protocol for evaluation and validation of TLR8 antagonists in HEK-Blue cells via secreted embryonic alkaline phosphatase assay. STAR Protoc. 2022;3(1):101061.

49. Lotz S, Aga E, Wilde I, van Zandbergen G, Hartung T, Solbach W, et al. Highly purified lipoteichoic acid activates neutrophil granulocytes and delays their spontaneous apoptosis via CD14 and TLR2. J Leukoc Biol. 2004 Mar;75(3):467–77.

50. Colombo I, Sangiovanni E, Maggio R, Mattozzi C, Zava S, Corbett Y, et al. HaCaT Cells as a Reliable in Vitro Differentiation Model to Dissect the Inflammatory/Repair Response of Human Keratinocytes. Mediators Inflamm. 2017;2017.

51. Micallef L, Belaubre F, Pinon A, Jayat-Vignoles C, Delage C, Charveron M, et al. Effects of extracellular calcium on the growth-differentiation switch in immortalized keratinocyte HaCaT cells compared with normal human keratinocytes. Exp Dermatol. 2009;18(2):143–51.

52. Boukamp P, Petrussevska RT, Breitkreutz D, Hornung J, Markham A, Fusenig NE. Normal keratinization in a spontaneously immortalized aneuploid human keratinocyte cell line. Journal of Cell Biology. 1988;106(3):761–71.

53. Deyrieux AF, Wilson VG. In vitro culture conditions to study keratinocyte differentiation using the HaCaT cell line. Cytotechnology. 2007;54(2):77–83.

54. Bosshart H, Heinzelmann M. THP-1 cells as a model for human monocytes. Ann Transl Med. 2016;4(21):4–7.

55. Marcantonini G, Zatini L, Costa S, Passerini M, Rende M, Luca G, et al. Natural Cryoprotective and Cytoprotective Agents in Cryopreservation: A Focus on Melatonin. Molecules. 2022; 27:1–17.

56. Mahmood T, Yang PC. Western blot: Technique, theory, and trouble shooting. N Am J Med Sci. 2012;4(9):429–34.

57. Vilkhovoy M, Adhikari A, Vadhin S, Varner JD. The evolution of cell free biomanufacturing. Processes. 2020;8(6):1–19.

58. Brady PN, Macnaughtan MA. Evaluation of Colorimetric Assays for Analyzing Reductively Methylated Proteins: Biases and1. Brady, P. N. & Macnaughtan, M. A. Evaluation of Colorimetric Assays for Analyzing Reductively Methylated Proteins: Biases and Mechanistic Insights. Physiol. Beha. Physiol Behav. 2017;176(10):139–48.

59. InvivoGen. QUANTI-Blue: Alkaline phosphatase detection reagent. San Diego: InvivoGen; 2024 [cited 2024 Nov 4].

60. Sakamoto S, Putalun W, Vimolmangkang S, Phoolcharoen W, Shoyama Y, Tanaka H, et al. Enzyme-linked immunosorbent assay for the quantitative/qualitative analysis of plant secondary metabolites. J Nat Med. 2018 Jan;72(1):32–42.

61. Leifer CA, Medvedev AE. Molecular mechanisms of regulation of Toll-like receptor signaling. J Leukoc Biol. 2016 Nov;100(5):927–41.

62. Singh A, Raju R, Mrad M, Reddell P, Münch G. The reciprocal EC50 value as a convenient measure of the potency of a compound in bioactivity-guided purification of natural products. Fitoterapia. 2020; 143:104598.

63. InvivoGen. HEK-Blue™ hTLR4 Cells Validation Data. San Diego: InvivoGen; 2023.

64. Petushkova NA, Rusanov AL, Pyatnitskiy MA, Larina O V., Zgoda VG, Lisitsa A V., et al. Proteomic characterization of HaCaT keratinocytes provides new insights into changes associated with SDS exposure. Biomedical Dermatology. 2020;4(1):1–13.

65. Park M, Woo SY, Cho KA, Cho MS, Lee KH. PD-L1 produced by HaCaT cells under polyinosinic-polycytidylic acid stimulation inhibits melanin production by B16F10 cells. PLoS One. 2020;15(5):1–10.

66. Alan A, Alan E, Arslan K, Daldaban F, Aksel EG, Çınar MU, et al. LPS- and LTA-Induced Expression of TLR4, MyD88, and TNF-α in Lymph Nodes of the Akkaraman and Romanov Lambs. Microscopy and Microanalysis. 2022;28(6):2078–2092.

67. Hu J, Wang G, Liu X, Zhou L, Jiang M, Yang L. Polo-Like Kinase 1 (PLK1) Is Involved in Toll-like Receptor (TLR)-Mediated TNF-α Production in Monocytic THP-1 Cells. PLoS One. 2013;8(10):4–11.

68. Zhang J, Zheng Q, Lu H, Jin F, Li Y, Bi F, et al. Notoginsenoside R1 protects human keratinocytes HaCaT from LPS-induced inflammatory injury by downregulation of Myd88. Int J Immunopathol Pharmacol. 2019; 33:20587.

69. Pivarcsi A, Bodai L, Réthi B, Kenderessy-Szabó A, Koreck A, Széll M, et al. Expression and function of Toll-like receptors 2 and 4 in human keratinocytes. Int Immunol. 2003 Jun 1;15(6):721–30.

70. Liu T, Huang T, Li J, Li A, Li C, Huang X, et al. Optimization of differentiation and transcriptomic profile of THP-1 cells into macrophage by PMA. PLoS One. 2023;18(7 July):1–14.

71. Hook JS, Patel PA, O'Malley A, Xie L, Kavanaugh JS, Horswill AR, et al. Lipoproteins from Staphylococcus aureus Drive Neutrophil Extracellular Trap Formation in a TLR2/1- and PAD-Dependent Manner. The Journal of Immunology. 2021;207(3):966–73.

72. van Bergenhenegouwen J, Kraneveld AD, Rutten L, Garssen J, Vos AP, Hartog A. Lipoproteins attenuate TLR2 and TLR4 activation by bacteria and bacterial ligands with differences in affinity and kinetics. BMC Immunol. 2016;17(1):1–10.

73. Rodrigues A, Queiróz DBC, Honda L, Silva EJR, Hall SH, Avellar MCW. Activation of Toll-Like Receptor 4 (TLR4) by In Vivo and In Vitro Exposure of Rat Epididymis to Lipopolysaccharide from Escherichia Coli1. Biol Reprod. 2008 Dec 1;79(6):1135–47.

74. Piktel E, Wnorowska U, Cieśluk M, Deptula P, Pogoda K, Misztalewska-Turkowicz I, et al. Inhibition of inflammatory response in human keratinocytes by magnetic nanoparticles functionalized with PBP10 peptide derived from the PIP2-binding site of human plasma gelsolin. J Nanobiotechnology. 2019;17(1):1–19.

75. Jiang Y, Tsoi LC, Billi AC, Ward NL, Harms PW, Zeng C, et al. Cytokinocytes: The diverse contribution of keratinocytes to immune responses in skin. JCI Insight. 2020;5(20).

76. Mestrallet G, Rouas-Freiss N, LeMaoult J, Fortunel NO, Martin MT. Skin Immunity and Tolerance: Focus on Epidermal Keratinocytes Expressing HLA-G. Front Immunol. 2021;12(December):1–10.

77. van Kesse KPM, Bestebroer J, van Strijp JAG. Neutrophil-mediated phagocytosis of Staphylococcus aureus. Front Immunol. 2014;5(SEP):1–12.

78. Gupta E, Kumar S, Srivastava VK, Saxena J, Siddiqui AJ, Mehta S, et al. Unravelling the Differential Host Immuno-Inflammatory Responses to Staphylococcus aureus and Escherichia coli Infections in Sepsis. Vaccines (Basel). 2022;10(10).